arXiv:1106.3125v2 [cond-mat.mes-hall] 25 Nov 2011

Chern semimetal and Quantized Anomalous Hall Effect in $HgCr_2Se_4$

Gang Xu, Hongming Weng, Zhijun Wang, Xi Dai, Zhong Fang
Beijing National Laboratory for Condensed Matter Physics, and Institute of Physics, Chinese Academy of Sciences, Beijing 100190, China;
(Dated: November 28, 2011)

In 3D momentum space, a topological phase boundary separating the Chern insulating layers from normal insulating layers may exist, where the gap must be closed, resulting in a "Chern semimetal" state with topologically unavoidable band crossings at the fermi level. This state is a condensed-matter realization of Weyl fermions in (3+1) D, and should exhibit remarkable features, such as magnetic monopoles and fermi arcs. Here we predict, based on first-principles calculations, that such a novel quantum state can be realized in a known ferromagnetic compound $HgCr_2Se_4$, with a single pair of Weyl fermions separated in momentum space. The quantum Hall effect without an external magnetic field can be achieved in its quantum-well structure.

PACS numbers: 71.20.-b, 73.20.-r, 73.43.-f

Under broken time reversal symmetry, the topological phases of two-dimensional (2D) insulators can be characterized by an integer invariant, called Chern number [1], which is also known as the TKNN number [2] or the number of chiral edge states [3] in the context of the quantum Hall effect. 2D insulators can thus be classified as normal insulators or Chern insulators depending on whether or not the Chern number vanishes. Since the Chern invariant is defined only for 2D insulators, it is natural to ask what is its analog in 3D? Starting from a 2D Chern insulating plane (say at $k_z = 0$), and considering its evolution as a function of k_z, generally two situations may happen. If the dispersion along k_z is weak, such that the Chern number remains unchanged, the system can be viewed as the simple stacking of 2D Chern insulating layers along the z direction. Such 3D Chern insulators are trivial generalization of the Chern number to 3D, which is quite similar to the weak topological insulators in systems with time reversal symmetry. However, if the dispersion along k_z is strong, such that Chern number changes as the function of k_z, the system will be in a nontrivial semimetal state with "topologically unavoidable" band crossings located at the phase boundary separating the insulating layers in $\vec{k}$ space with different Chern numbers [4, 5]. This is due to the fact that the change of Chern number corresponds to a topological phase transition, which can happen only if the gap is closed. From the Kohn-Luttinger theorem, we can always expect that the band crossings appear at the fermi level at stoichiometry.

This Chern semimetal state, if found to exist, can be regarded as a condensed matter realization of (3+1)D chiral fermions (or called Weyl fermions) in the relativistic quantum field theory, where the field can be described by the 2-component Weyl spinors [6] (either left- or right-handed), which are half of the Dirac spinors and must appear in pairs. The band-crossing points or Weyl nodes are topological objects in the following senses. First, since no mass is allowed in 2×2 Hamiltonian, the Weyl nodes should be locally stable and can only be removed when a pair of Weyl nodes meet together in the $\vec{k}$ space. Second the Weyl nodes are "topological defects" of the gauge field associated with the Berry's curvature in momentum space [7–9]. The gauge field around the neighborhood of the Weyl node must be singularly enhanced, and behaves like magnetic field originating from a magnetic monopole [8]. The physical consequence of such a gauge field has been discussed in the context of anomalous Hall effect [7, 8, 10] observed in ferromagnetic (FM) metals, where the Weyl nodes, if any, are always submerged by the complicated band structures.

In this Chern semimetal state, we may also expect unusual features like non-closed fermi surfaces (fermi arcs) on the side surfaces. The possible fermi arcs have been recently discussed from a view point of accidental degeneracy, and prospected for non-collinear antiferromagnetic pyrochlore iridates [11] by the fine-tuning of electron correlation U. Since the correct U and the real magnetic ordering is still unknown, we have to wait for its material realization. In this paper, we will show that such a novel Chern semimetal state is actually realized as the ground state of a known FM material $HgCr_2Se_4$, with only a single pair of Weyl nodes separated in the momentum space. We further find that the long-pursuing quantized anomalous Hall effect (QAHE) [12–15], i.e., the quantum Hall effect without an external magnetic field, can be achieved in the quantum-well structure of $HgCr_2Se_4$.

$HgCr_2Se_4$ is a FM spinel exhibiting large coupling effects between electronic and magnetic properties [16]. It shows novel properties like giant magnetoresistance [17], anomalous Hall effect [18], and red shift of optical absorption edge [19]. Its Curie temperature T_c is high (around 106∼120 K), and its saturated moment is 5.64 μ_B/f.u. [20, 21], approaching the atomic value expected for high-spin Cr^{3+}. Its transport behavior is different from other FM chalcogenide spinels, like $CdCr_2Se_4$ and $CdCr_2S_4$ which are clearly semiconducting. $HgCr_2Se_4$ exhibits semiconducting character in the paramagnetic state but metallic in the low temperature FM phase [17,

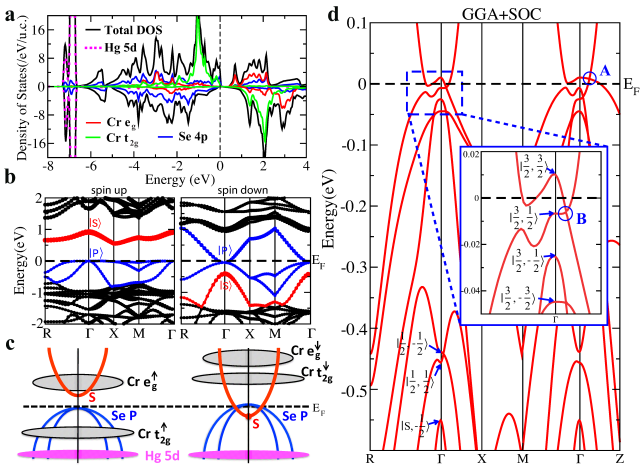

FIG. 1: (Color online) **Electronic Structures of $HgCr_2Se_4$.** (a) The total and partial density of states (DOS); (b) The band structures without SOC (showing the up and down spin parts separately); (c) The schematic understanding for the band-inversion, where the $|S\rangle$ state is lower than the $|P\rangle$ states in the down spin channel; (d) The band structure after including SOC (with majority spin aligning to the (001) direction). The low energy states at Γ are indicated as explained in the main text.

22, 23]. The spinel structure (space group $Fd\bar{3}m$) can be related to the zinc-blende and diamond structures in the following way. If we treat the Cr_2Se_4 cluster as a single pseudo-atom (called X) located at its mass-center, then the HgX sublattice forms a zinc blende structure. There are two HgX sublattices in each unit cell, and they are connected by the inversion symmetry similar to the two atoms in the diamond structure. The pseudo atom X is actually a small cube formed by Cr and Se atoms located at the cube corners. The cubes are connected by corner sharing the Cr atoms. As the result, each Cr atom is octahedrally coordinated by 6 nearest Se atoms.

Our first-principles calculations [24] confirm that FM solution is considerably (2.8eV/f.u.) more stable than non-magnetic solution, and the calculated moment (6.0 μ_B/f.u) is in good agreement with experiments [20, 21]. The electronic structures shown in Fig.1(a) and (b) suggest that the system can be approximately characterized as a "zero-gap half-metal" in the case without spin-orbit coupling (SOC). It is almost a half-metal because of the presence of a gap in the up-spin channel just above the Fermi level; it is nearly zero-gapped because of the band-touching around the Γ point just below Fermi level in the down spin channel. The 3d-states of Cr^{3+} are strongly spin-polarized, resulting in the configuration $t_{2g}^{3\uparrow}e_g^{0\uparrow}t_{2g}^{0\downarrow}e_g^{0\downarrow}$. The octahedral crystal field surrounding Cr atoms is strong and opens up a band gap between the $t_{2g}^{3\uparrow}$ and $e_g^{0\uparrow}$ manifolds. The Se-4p states (located from about -6 eV to 0 eV) are almost fully occupied and contribute to the valence band top dominantly. Due to the hybridization with Cr-3d states, the Se-4p are slightly spin-polarized but with opposite moment (about -0.08 μ_B/Se). The zero-gap behavior in down spin channel is the most important character here (Fig.1(b)), because it suggests the inverted band structure around the Γ point, similar to the case of HgSe or HgTe [25, 26].

The four low energy states (8 after considering spin) at the Γ point can be identified as $|P_x\rangle$, $|P_y\rangle$, $|P_z\rangle$, and $|S\rangle$, which are linear combinations of atomic orbitals [27]. Considering these 4 states as basis, we now recover the same situation as HgSe or HgTe, and the only difference is the presence of exchange splitting in our case. Here the band inversion (see Fig.1(c), $|S,\downarrow\rangle$ is lower than $|P,\downarrow\rangle$) is due to the following two factors. First, the Hg-5d states are very shallow (located at about -7.0 eV, Fig.1(a)) and its hybridization with Se-4p states will push the anti-bonding Se-4p states higher, similar to HgSe. In addition to that, the hybridization between unoccupied Cr-3$d^{\downarrow}$ and Hg-6$s^{\downarrow}$ states in the down spin channel will push the Hg-6$s^{\downarrow}$ state lower in energy (Fig.1(b) and (c)). As the results, the $|S,\downarrow\rangle$ is about 0.4eV lower than $|P,\downarrow\rangle$ states, and it is further enhanced to be 0.55eV in the presence of SOC. We have to be aware of the correlation effect beyond GGA, because the higher the Cr-3$d^{\downarrow}$ states, the weaker the hybridization with Hg-6$s^{\downarrow}$. It has been shown that semiconducting $CdCr_2S_4$ and $CdCr_2Se_4$ can be well described by the LDA+U calculations with effective U around 3.0 eV [28, 29]. We have performed the same LDA+U calculations for $HgCr_2Se_4$ and found that the band-inversion remains unless the U is unreasonably large (> 8.0 eV). The experimental observations of metallic behavior at low temperature for all kinds of samples [17, 22, 23] are strong supports to our conclusion for the inverted band structure.

In the presence of SOC, the new low energy eigen states at Γ are given as $|\frac{3}{2},\pm\frac{3}{2}\rangle$, $|\frac{3}{2},\pm\frac{1}{2}\rangle$, $|\frac{1}{2},\pm\frac{1}{2}\rangle$, and $|S,\pm\frac{1}{2}\rangle$, which can be constructed from the $|P\rangle$ and $|S\rangle$ states [31], similar to HgSe again. Now because of the exchange splitting in our case, the eight states at Γ are all energetically separated, with the $|\frac{3}{2},\frac{3}{2}\rangle$ having the highest energy, and the $|S,-\frac{1}{2}\rangle$ being the lowest. Due to the band-inversion, several band-crossings are observed as shown in the band structure (Fig.1(d)). Among them, however, only two kinds of band-crossings (called A and B) are important for the states very close to the Fermi level. The crossing-A gives two points located at $k_z = \pm k_z^c$ along the $\Gamma - Z$ line, and the trajectory of crossing-B is a closed loop surrounding Γ point in the k_z=0 plane, as schematically shown in Fig.2(a). For the 2D planes with fixed-k_z ($k_z \neq 0$ and $k_z \neq \pm k_z^c$), the band structures are all gapped (in the sense that we can define a curved fermi level). We can therefore evaluate its Chern number C for each k_z-fixed plane. We found that $C = 0$ for the planes with $k_z < -k_z^c$ or $k_z > k_z^c$, while $C = 2$ for the planes with $-k_z^c < k_z < k_z^c$ and $k_z \neq 0$. We therefore conclude that the crossing-A located at the phase boundary be-

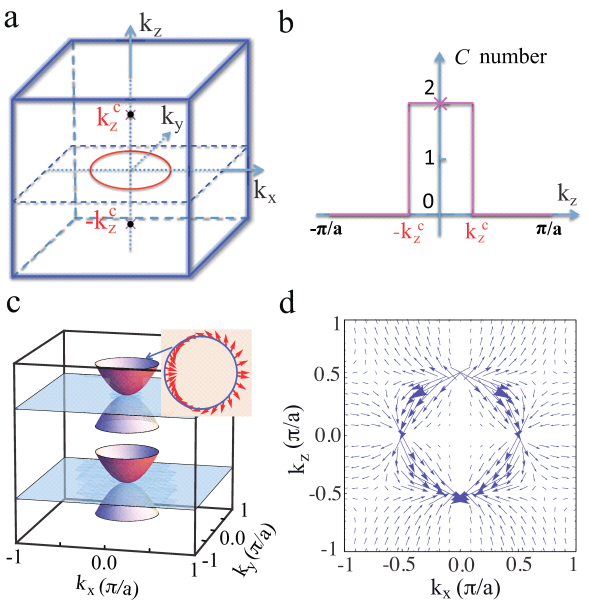

FIG. 2: (Color online) **Weyl nodes and gauge flux in $HgCr_2Se_4$** (a) The band-crossing points in the $\vec{k}$-space; (b) The Chern number as function of k_z; (c) The schematic plot of the band dispersion around the Weyl nodes in the k_z=$\pm k_z^c$ plane, and the inset shows the chiral spin texture. (d) The gauge flux evaluated as Berry curvature in the (k_x, k_z) plane.

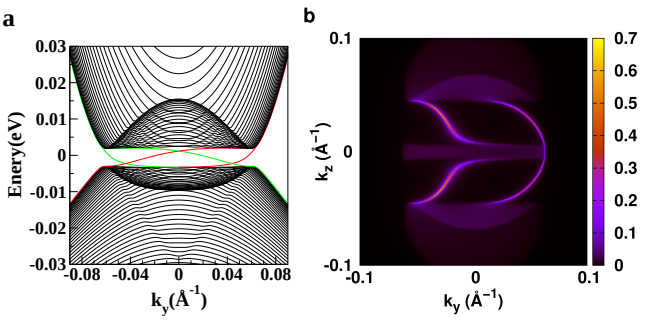

FIG. 3: (Color online) **Edge states and Fermi arcs of $HgCr_2Se_4$ [31].** (a) The edge states for the plane with k_z=0.06π. A ribbon with two edges is used, and there are two edge states for each edge (because C=2). The states located at different edges are indicated by different colors. (b) The calculated Fermi arcs for the (k_y,k_z) side surface.

tween $C = 2$ and $C = 0$ planes (i.e, at $k_z = \pm k_z^c$) are topologically unavoidable Weyl nodes as addressed at the beginning. On the other hand, however, the crossing-B (i.e, the closed loop in $k_z = 0$ plane) is just accidental and it is due to the presence of crystal mirror symmetry with respect to the k_z=0 plane. The crossing-B is not as stable as crossing-A in the sense that it can be eliminated by changing the crystal symmetry.

Using the 8 eigen states at Γ, we can construct an 8×8 effective $\mathbf{k}\cdot\mathbf{p}$ Kane-Hamiltonian [31]. For qualitative understanding, however, we can downfold the 8×8 Hamiltonian into a simplest 2×2 model by considering the two basis $|\frac{3}{2}, \frac{3}{2}\rangle$ and $|S, -\frac{1}{2}\rangle$ which catch the band-inversion nature.

$$H_{eff} = \begin{bmatrix} M & Dk_zk_-^2 \\ Dk_zk_+^2 & -M \end{bmatrix} \qquad (1)$$

here $k_\pm = k_x \pm ik_y$, and $M = M_0 - \beta k^2$ is the mass term expanded to the second order, with parameters $M_0 > 0$ and $\beta > 0$ to ensure band inversion. Since the two basis have opposite parity, the off-diagonal element has to be odd in k. In addition, the $k_\pm^2$ has to appear to conserve the angular moment along z-direction. Therefore, to the leading order, the $k_zk_\pm^2$ is the only possible form for the off-diagonal element. Evaluating the eigen values $E(k) = \pm\sqrt{M^2 + D^2k_z^2(k_x^2 + k_y^2)^2}$, we get two gapless solutions: one is the degenerate points along the $\Gamma - Z$ line with $k_z = \pm k_z^c = \pm\sqrt{M_0/\beta}$; the other is a circle around the Γ point in the $k_z = 0$ plane determined from the equation $k_x^2 + k_y^2 = M_0/\beta$. They are exactly the band-crossings obtained from our first-principles calculations. Due to the presence of $k_\pm^2$ in the off-diagonal element [30], it is easy to check that Chern number C equals to 2 for the planes with $-k_z^c < k_z < k_z^c$ and $k_z \neq 0$. The band dispersions near the Weyl nodes at $k_z = \pm k_z^c$ plane (Fig.2(c)) are thus quadratic rather than linear, with chiral in-plane spin texture (shown in the inset of Fig.2(c)). The two Weyl nodes located at $\pm k_z^c$ have opposite chirality due to the opposite sign of mass term, and they form a single pair of magnetic monopoles carrying gauge flux in $\vec{k}$-space as shown in Fig.2(d). The band-crossing loop in the $k_z = 0$ plane is not topologically unavoidable, however, its existence requires that all gauge flux in the k_z=0 plane (except the loop itself) must be zero.

This Chern semi-metal state realized in $HgCr_2Se_4$ will lead to novel physical consequences, which can be measured experimentally. First, each k_z-fixed plane with non-zero Chern number can be regarded as a 2D Chern insulator, and there must be chiral edge states for such plane if an edge is created. The number of edge states is two for the case of C=2 (see Fig.3(a)), or zero for the case of C=0. If the chemical potential is located within the gap, only the chiral edge states can contribute to the fermi surface, which are isolated points for each Chern insulating plane but nothing for the plane with C=0. Therefore the trajectory of such points in the (k_x, k_z) surface or (k_y, k_z) surface form non-closed fermi arcs, which can be measured by ARPES. As shown in Fig.3(b), the fermi arcs end at k_z=$\pm k_z^c$, and are interrupted by the k_z=0 plane. This is very much different from conventional metals, where the fermi surfaces must be either closed or interrupted by the Brillouin zone boundary. The possible fermi arcs has been recently discussed from a view point of accidental degeneracy for pyrochlore iridates [11]. Nevertheless, for the Chern semi-metal state, the fermi arcs should be more stable because the band-

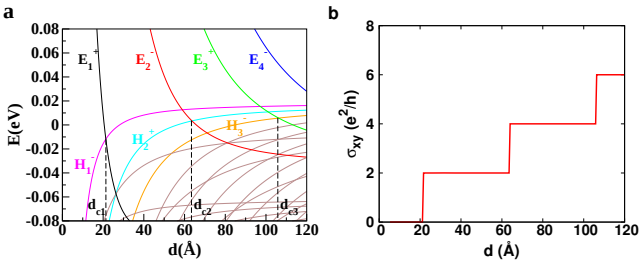

FIG. 4: (Color online) **Quantized Anomalous Hall effect in $HgCr_2Se_4$ thin film [31].** (a) The subband energy levels at Γ point as function of film thickness. (b) The Hall conductance as function of film thickness.

crossings are topologically unavoidable.

The QAHE, on the other hand, is an unique physical consequence characterizing the Chern semi-metal nature of $HgCr_2Se_4$, by considering its quantum-well structure. For 2D Chern insulators, the transverse Hall conductance should be quantized as $\sigma_{xy} = C\frac{e^2}{h}$, where C is the Chern number. Such a quantum Hall effect without magnetic field has been long-pursued [12, 13, 15] but never achieved experimentally. In $HgCr_2Se_4$, considering the k_z-fixed planes, the Chern number C is non-zero for limited regions of k_z, and this is due to the band inversion around Γ as discussed above. In the quantum well structure, however, those low energy states around Γ should be further quantized into subbands (labeled as $|H_n\rangle$ and $|E_n\rangle$ for hole and electron subbands respectively), whose energy levels change as function of film thickness. As shown in Fig.4(a), when the thickness of the film is thin enough the band inversion in the bulk band structure will be removed entirely by the finite size effect. With the increment of the film thickness, finite size effect is getting weaker and the band inversion among these subbands restores subsequently, which leads to jumps in the Chern number or the Hall coefficient σ_{xy} [14]. As shown in Fig.4(b), if the film is thinner than 21Å(about 2 lattice constants), the σ_{xy} is zero; once the film thickness is larger than the critical thickness, we find subsequent jumps of σ_{xy} in unit of $2e^2/h$. In fact, the strong anomalous Hall effect has been observed for the bulk samples of $HgCr_2Se_4$ [18]. This is in sharp contrast with pyrochlore iridates, where the anomalous Hall effect should be vanishing due to the AF ordering.

We acknowledge the valuable discussions with Y. Ran, A. Bernevig, and the supports from NSF of China and that from the 973 program of China (No.2007CB925000).

[1] D. J. Thouless, *Topological Quantum Numbers in Nonrelativistic Physics* (World Scientific, Singapore, 1998).
[2] D. J. Thouless, M. Kohmoto, M. P. Nightingale, and M. den Nijs, Phys. Rev. Lett. **49**, 405 (1982).
[3] B. I. Halperin, Phys. Rev. B **25**, 2185 (1982).
[4] T. Thonhauser, D. Vanderbilt, Phys. Rev. Lett., **74**, 235111 (2006).
[5] T. Hughes, E. Prodan, B. A. Bernevig, arXiv: cond-matt/1010.4508 (2010).
[6] H. Weyl, Z. Phys., **56**, 330 (1929).
[7] T. Jungwirth, Q. Niu, and A. H. MacDonald, Phys. Rev. Lett. **88**, 207208 (2002).
[8] Z. Fang, et.al., SCIENCE, **302**, 92 (2003).
[9] G. E. Volovik, JETP Lett., **75**, 55 (2002).
[10] N. Nagaosa, J. Sinova, S. Onoda, A. H. MacDonald, N. P. Ong, Rev. Mod. Phys. **82**, 1539 (2010).
[11] X. G. Wan, A. M. Turner, A. Vishwanath, S. Y. Savrasov, Phys. Rev. B **83**, 205101 (2011).
[12] F. D. M. Haldane, Phys. Rev. Lett. **61**, 2015 (1988).
[13] M. Onoda, N. Nagaosa, Phys. Rev. Lett. **90**, 206601 (2003).
[14] C. X. Liu, X. L. Qi, X. Dai. Z. Fang, S. C. Zhang, Phys. Rev. Lett. **101**, 146802 (2008).
[15] R. Yu, W. Zhang, H. J. Zhang, S. C. Zhang, X. Dai, Z. Fang, Science, **329**, 61 (2010).
[16] P. J. Wojtowicz, IEEE Trans. on Magn., **5**, 840 (1969).
[17] N. I. Solin, V. V. Ustinov, S. V. Naumov, Phys. Solid State, **50**, 901 (2008).
[18] N. I. Solin, N. M. Chebotaev, Phys. Solid State, **39**, 754 (1997).
[19] T. Arai, M. Wakaki, S. Onari, K. Kubdo, T. Satoh, T. Tsushima, J. Phs. Soc. Jpn. **34**, 68 (1973).
[20] P. K. Baltzer, H. W. Lehmann, M. Robbins, Phys. Rev. Lett. **15**, 493 (1965).
[21] P. K. Baltzer, P. J. Wojtowicz, M. Robbins, E. Lopatin, Phys. Rev **151**, 367 (1966).
[22] H. W. Lehmann, F. P. Emmenegger, Solid State Comm. **7**, 965 (1969).
[23] A. Selmi, A. Mauger, M. Heritier, J. Mag. Mag. Mat., **66**, 295 (1987).
[24] We used the WIEN2k package with the generalized gradient approximation (GGA). The experimental structure parameters [21] are used, and the Brillouin zone is sampled with 11×11×11 k-point mesh.
[25] A. Delin, Phys. Rev. B **65**, 153205 (2002).
[26] C. Y. Moon, S. H. Wei, Phys. Rev. B **74**, 045205 (2006);
[27] The low energy states are: $|P_\alpha\rangle \approx \frac{1}{\sqrt{8}}\sum_{i=1}^{8}|p_\alpha^i\rangle$, and $|S\rangle \approx 0.4\sum_{j=1}^{2}|s^j\rangle + 0.24\sum_{k=1}^{4}|d_{t_{2g}}^k\rangle$, where $\alpha = x, y, z$, and i, j, k runs over Se, Hg, Cr atoms in the unit cell respectively; $|s\rangle$, $|p_{\alpha=x,y,z}\rangle$, $|d_{t_{2g}=xy,yz,zx}\rangle$ are corresponding atomic orbitals of each atom.
[28] C. J. Fennie, K. M. Rabe, Phys. Rev. B **72**, 214123 (2005).
[29] A. N. Yaresko, Phys. Rev. B **77**, 115106 (2008).
[30] M. Onoda, N. Nagaosa, J. Phys. Soc. Jpn. **71**, 19 (2002).
[31] Lok C. Lew Yan Voon, M. Willatzen, *The kp method: Electronic Properties of Semiconductors*, (Springer, Berlin, 2009). See pages 57-58 for the definition of basis and 8-bands Kane-Hamiltonian. The parameters fitted to our first-principles calculations are given as E_0=0.174eV, Δ_0=0.352eV, P=2.592eVÅ, m_s=0.5424m_0 and m_p=-2.966m_0. Two more parameters, describing the exchange splitting of electron and valence bands, are h_s=0.666eV and h_p=0.040eV. Replacing k_x by $-i\hbar\partial_x$ and using open boundary condition, we can diagonalize the Hamiltonian for each fixed-k_z, and obtain the edge states. If we consider the open boundary condition along z direction, us-

ing the same strategy, we can evaluate the Hall conductance in the quantum well structure. The QAHE is further confirmed by tight-binding calculations constructed from maximumly localized wannier functions.